AD-A132 699 LOW FREQUENCY RAMAN SPECTRA OF V-B2O3 AS A FUNCTION OF TEMPERATURE AND PRESSURE(U) HOWARD UNIV WASHINGTON DC DEPT OF CHEMISTRY S GUHA ET AL. 08 SEP 83 TR-16 1/1

UNCLASSIFIED N00014-80-C-0305 F/G 7/4 NL

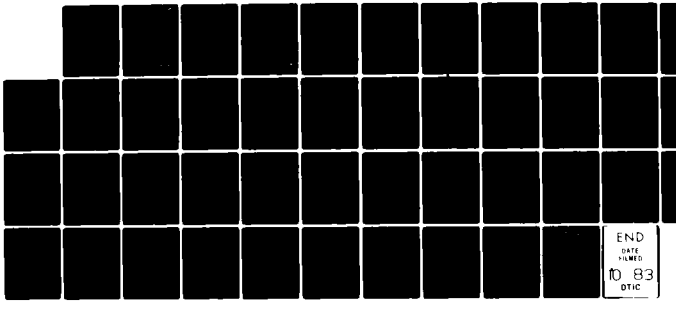

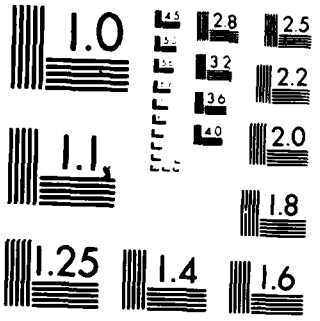

AD-A132 699

DTIC FILE COPY

SECURITY CLASSIFICATION OF THIS PAGE (When Data Entered)

REPORT DOCUMENTATION PAGE		READ INSTRUCTIONS BEFORE COMPLETING FORM
1. REPORT NUMBER: 16	2. GOVT ACCESSION NO.: AD-A132 699	3. RECIPIENT'S CATALOG NUMBER:
4. TITLE (and Subtitle): Low Frequency Raman Spectra of v-B_2O_3 As a Function of Temperature And Pressure		5. TYPE OF REPORT & PERIOD COVERED: Technical Report #16
		6. PERFORMING ORG. REPORT NUMBER:
7. AUTHOR(s): Soumyendu Guha, and George E. Walrafen		8. CONTRACT OR GRANT NUMBER(s): N00014-80-C-0305
9. PERFORMING ORGANIZATION NAME AND ADDRESS: Department of Chemistry, Howard University, Washington, D.C. 20059		10. PROGRAM ELEMENT, PROJECT, TASK AREA & WORK UNIT NUMBERS: NR-051-733
11. CONTROLLING OFFICE NAME AND ADDRESS: Office of Naval Research, Department of the Navy, Arlington, Virginia 22217		12. REPORT DATE: September 8, 1983
		13. NUMBER OF PAGES: 47
14. MONITORING AGENCY NAME & ADDRESS(if different from Controlling Office)		15. SECURITY CLASS. (of this report): Unclassified
		15a. DECLASSIFICATION/DOWNGRADING SCHEDULE:

16. DISTRIBUTION STATEMENT (of this Report)

Approved for public release; reproduction is permitted fro any purpose of the United States government distribution is unlimited.

17. DISTRIBUTION STATEMENT (of the abstract entered in Block 20, if different from Report)

Distribution of this document is unlimited

18. SUPPLEMENTARY NOTES

Prepared and accepted for publication in the Journal of Chemical Physics.

19. KEY WORDS (Continue on reverse side if necessary and identify by block number)

Raman Scattering, B_2O_3 Galss, Temperature Dependence, Low Frequency Peak, Low Temperature

20. ABSTRACT (Continue on reverse side if necessary and identify by block number)

SEE REVERSE SIDE FOR ABSTRACT

DD FORM 1 JAN 73 1473 EDITION OF 1 NOV 65 IS OBSOLETE
S/N 0102-014-6601

SECURITY CLASSIFICATION OF THIS PAGE (When Data Entered)

ABSTRACT

Raman studies of vitreous B_2O_3 have been conducted between 8 and 700K, and as a function of hydrostatic pressure (~8 kbar) at room temperature. The low temperature Raman spectra exhibit two broad bands at 50 cm^{-1} and 137 cm^{-1}. From the temperature dependence of the 50 cm^{-1} band, it has been concluded that the vibrational density of states in the low frequency region ($30<\omega<300$ cm^{-1}) is better described when the Raman coupling coefficient C_b varies as ω . A shift in frequency of the Raman spectra as a function of temperature is attributed to a structural change near the glass transition. It is postulated that at room temperature, the structure of v-B_2O_3 is comprised of an equal proportion of boroxol (B_3O_6) rings and BO_3 triangles. The low frequency vibrational band at 50 cm^{-1} arises from a cooperative motion of random distributions of mass of various shapes and sizes in the B_2O_3 glass. Near the glass transition temperature, the boroxol rings break up thereby leading to a more open structure. Above the melting point, i.e. when the viscosity is low, a regrouping of atoms occurs which results in a low density random network structure of BO_3 triangles. The mode Gruneisen constants obtained from the high pressure Raman data are found to be +3.42 and -2.05 for the two bands. The observed positive and negative values of γ lend support to our proposed model in which we assign the 137 cm^{-1} band to the librational motion of boroxol rings.

LOW FREQUENCY RAMAN SPECTRA OF v-B_2O_3 AS A FUNCTION OF TEMPERATURE AND PRESSURE

by

Soumyendu Guha and George E. Walrafen

Chemistry Department

Howard University

Washington, D.C. 20059

This work was supported by contracts from Office of Naval Research

ABSTRACT

Raman studies of vitreous B_2O_3 have been conducted between 8 and 700K, and as a function of hydrostatic pressure (~ 8 kbar) at room temperature. The low temperature Raman spectra exhibit two broad bands at 50 cm^{-1} and 137 cm^{-1}. From the temperature dependence of the 50 cm^{-1} band, it has been concluded that the vibrational density of states in the low frequency region ($30<\omega<300$ cm^{-1}) is better described when the Raman coupling coefficient C_b varies as ω . A shift in frequency of the Raman spectra as a function of temperature is attributed to a structural change near the glass transition. It is postulated that at room temperature, the structure of v-B_2O_3 is comprised of an equal proportion of boroxol (B_3O_6) rings and BO_3 triangles. The low frequency vibrational band at 50 cm^{-1} arises from a cooperative motion of random distributions of mass of various shapes and sizes in the B_2O_3 glass. Near the glass transition temperature, the boroxol rings break up thereby leading to a more open structure. Above the melting point, i.e. when the viscosity is low, a regrouping of atoms occurs which results in a low density random network structure of BO_3 triangles. The mode Gruneisen constants obtained from the high pressure Raman data are found to be +3.42 and -2.05 for the two bands. The observed positive and negative values of γ lend support to our proposed

model in which we assign the 137 cm^{-1} band to the librational motion of boroxol rings.

I. Introduction

Raman studies of vitreous and molten B_2O_3 have been conducted by various investigators.[1-10] In these investigations, the structure of vitreous B_2O_3 was explained primarily from a vibrational feature at 806 cm^{-1} in the Raman spectrum. For quite sometime, it has been considered that boroxol rings are major consitituents of the structure, and the 806 cm^{-1} peak has been attributed to vibrations associated with the B_3O_6 groupings containing a six membered B_3O_6 ring. Recently, Windish and Risen[2] have demonstrated from isotopic substitutions of ^{11}B and ^{18}O, that the 806 cm^{-1} peak is associated with the localized oxygen motions of the B_3O_6 ring. It has also been observed[1] that the intensity of this peak starts decreasing at the glass transition temperature, and this is attributed to a rapid breakdown of boroxol rings with increasing temperature.

Although, a great deal of information has been obtained from the vibrational spectra of v-B_2O_3, very little is known about the nature and origin of a depolarized low frequency Raman peak at 26 cm^{-1}. A broad depolarized low frequency (< 300 cm^{-1}) Raman band is observed in most glasses. It is believed that this is a first order vibrational band, which arises from a breakdown in the $k=0$ Raman selection rule. A major problem arises in determining the density of vibrational states of vitreous materials from Raman data because it requires the knowledge of the coupling coefficient

C_b which is related to the Stokes spectrum shape as:[3]

$$I(\omega) = C_b[n(\omega)+1]\, g_b(\omega)/\omega \qquad (1)$$

where $n(\omega)$ is the Bose-Einstein population factor, $g_b(\omega)$ is the vibrational density of states of band b, and C_b is the coupling factor between the vibrational band (b) and the incident radiation. A temperature reduced Raman spectrum is defined as:

$$I^T(C_b-\omega) = I(\omega)/[n(\omega)+1] \qquad (2)$$

Shuker and Gammon[3a] found that for v-SiO_2, the temperature reduced Raman spectrum agreed well with the calculated density of states. This implies that C_b varies as ω. However, for a-Si, a-As_2S_3, a-GeS_2 and a-$GeSe_2$ [5], C_b was found to be proportional to ω^2. This was theoretically explained in the light of electrical or mechanical disorder of the vibrations due to a lack of periodicity of the atoms in amorphous materials. Although a low frequency Raman study of v-B_2O_3 has been reported before by Shuker and Gammon [3(b)], we present here a detailed study of v-B_2O_3 as a function of temperature between 4 and 700K. High pressure (~8 Kbar) room temperature Raman data will also be reported. The aim of this present investigation is to understand the nature and origin of the vibrational density of states in the low frequency region, explore the possibility of probing the stucture of v-B_2O_3 at different temperatures, and tentatively ascribe a dynamic motion to this structure at different temperatures. The outline of this paper is as follows:

In Section II, we describe the experimental procedures and techniques. In Section III, we report the experimental data and calculated vibrational density of states using equation (1) with a pre-assumed functional form of C_b. The validity of these functional forms of C_b (which are assumed as C_b^{-1}, ω and ω^2) to describe a vibrational density of states for v-B_2O_3 in the low frequency region (<300 cm^{-1}), will be discussed in section IV-A and IV-B. In section IV-C, we try to explain the origin of the low-frequency vibrational spectrum by proposing a possible structure of the B_2O_3 glass. This model-structure is further discussed in Section IV-C in terms of the glass-transition phenomenon. High pressure Raman data will be discussed in Section V.

II. Experimental

A. Sample preparation

For low temperature (<300K) experiments, samples of B_2O_3 glass were formed from melts using high purity (> 99.9%) B_2O_3, obtained from Apache Chemicals Inc. The melts were heated to 1000°C for 24 hours in a platinum crucible and then poured onto a cold surface. A sample of size (1/8 x 1/8 x 1/4") was prepared by first grinding to a rectangular shape and then polishing on a 1 μ lapping cloth. Because the sample was hygroscopic the polishing was done in a nitrogen atmosphere and was immediately transfered to the low temperature dewar, which

was then evacuated quickly to 1$^{\mu}$ pressure.

For high temperature (>300K) experiments, molten B_2O_3 was slowly cooled to room temperature in a platinum crucible. The same crucible was then heated up slowly in a small homemade furnace. A Pt, Pt-13% Rh thermocouple was inserted in the melt, close to the surface, and was firmly positioned when the melt was cooled down to room temperature. This enabled us to measure the surface temperature for back-scattering Raman experiments.

B. Raman Measurements

i. Low Temperature

Raman data were obtained with an Instruments SA double monochromator, which was interfaced with a Nicolet 1170 multi-channel analyzer. For detection, a cooled Hamamatsu R928P phototube was used. The discriminator output of a PAR 1140 quantum photometer was connected to the input of the Nicolet 1170. The data were stored in floppy discs and were analyzed with a HP87 computer.

The sample was mounted in a low temperature cold tip dewar, and a chromel/gold 0.07% iron thermocouple was used to measure the temperature which was monitored by an Air Products digital temperature controller. The thermocouple junction was placed very close to the sample and the accuracy of the measured

temperatures was ± 1K. The temperature of the sample was varied between 5 and 300K by resistive heating and was controlled by the temperature controller. A 90° scattering geometry was employed in the low temperature experiments. The scattered light was collected with an F/1.8 lens. A polarization scrambler was employed in low temperature experiments. The Raman spectra were recorded with the following geometries:(a) (VV) geometry, where the incident and scattered polarizations of the electric vector were oriented perpendicular to the scattering plane, which is defined as the plane containing the incident and scattered propagation directions;(b)(HV) geometry, in which the incident electric vector is parallel to the scattering plane,while the scattered electric vector is normal to the scattering plane. In the low frequency region, only the depolarized (HV) spectra are presented in this article. Green excitation (5145A) of approximately 100 mw laserpower was employed in all low temperature (<300K) measurements.

ii. High Temperature

The high temperature Raman data were obtained with a back scattering geometry. The incident laser light was focused through a 1/4" hole bored in a metal mirror (coated with Rh to withstand heat), which was positioned at a 45° angle facing the spectrometer.

The same mirror collected the scattered light off the solid sample surface and was then focused onto the slit by the collecting lens of the spectrometer. The incident light was allowed to reflect back through the hole of the mirror, thereby eliminating plasma lines. The sample was heated gradually from room temperature and Raman data were only recorded when the temperature was found to be stable within ± 10°C. The sample surface was flushed intermittently with nitrogen gas to keep it dry. Green (5145) excitation of approximately 500 mw of power was used. Because of the scattering geometry, only depolarized light measurements were conducted.

iii. High Pressure

The high pressure equipment consisted of an optical cell fitted with two sapphire windows and a 1:10 intensifier, both manufactured by Autoclave Engineers, Inc. Hydrostatic pressure was generated by means of a 2 Kbar hand pump. The hydraulic fluid (glycerol) was allowed to enter the cell through a 1/16" hole in the high pressure cell. A calibration graph between the low and high pressure at the two ends of the intensifier was obtained with a high pressure (165,000 PSI) Bourdon gauge connected at the entrance side of the optical pressure cell. During the experiment, high pressure values were solely determined

from this graph by monitoring the low pressure (30,000 PSI) gauge at the low pressure end of the intensifier.

A rectangular sample (~5 x 5 x 10 mm) was held in a cylindrical brass cell which had two 1/4" holes at its two ends and a rectangular slot perpendicular to its axis. This rectangular slot allowed us to insert the sample as well as to collect the scattered light. The sample faces were polished and then coated black except for the two sides which were used for allowing the laser beam in and the scattered light out of the sample. The brass cell was also coated black to minimize the reflected light. Green light (5145A) with approximately 500 mw power was used. The slit-width was set at 6 cm^{-1}. The Raman spectra were recorded in 90^{o} scattering geometry with VV and HV polarization; however only the depolarized (HV) spectra are presented here.

III. Experimental Results

The low frequency Raman data as a function of temperature are shown in Figure 1. At 8K, the two broad bands at 50 cm^{-1} (peak 1) and 137 cm^{-1} (peak 2) are observed, which are of primary interest in this investigation. The shift of peak 1 as a function of temperature is shown in Figure 2(a). Peak 1 gradually shifts to 28 cm^{-1} at 70K and remains constant up to 500K. It is further decreased to 10 cm^{-1} at 673K.

The gradual decrease in frequency of peak 1 between 8 and 70K is not observed in the temperature reduced Raman spectra (Figure 2(b) and Figure 3). The spectral density of states of the temperature reduced Raman spectra also indicates two bands at 50 cm^{-1} and 137 cm^{-1} between 8 and 500K. The peak position of the 50 cm^{-1} band shifts to 32 cm^{-1} between 500 and 673K as is shown in Figure 2(b).

The intensity of peak 2 at 137 cm^{-1} in the recorded Raman spectra was observed to be weak (~ 200 counts/sec as compared to ~ 5K counts/sec for peak 1 at room temperature) at all temperatures. Because of the broadness of this band and weakening of its intensity at higher temperatures, we find it difficult to associate a peak position with this band at each temperature. This is why we have not plotted the shift in frequency of peak 2 as a function of temperature.

Figures 4 and 5 are the frequency reduced Raman spectra. Following equation (1), the vibrational dansity of states $g_b(\omega)$ can be written as:

$$I^F(C_b) = g_b(\omega) = \frac{I(\omega)\ \omega}{C_b\ (n(\omega) + 1)} \qquad (3)$$

The frequency reduced Raman spectra are dependent on the coupling coefficient C_b. In Figure 4, the coefficient C_b is assumed to be ω^2, while in Figure 5, it is

1. For a future reference, we call them $I^F(C_b \sim \omega^2)$ and $I^F(C_b \sim 1)$ respectively.

It should be noted in Figure 4 that the spectral line shape is remarkably the same at all temperatures between 70 and 500K. Peak 1 occurs at 26 cm^{-1} and band 2 is centered at 137 cm^{-1}. The temperature dependence of peak 1 for the frequency reduced spectra $I^F(C_b \sim \omega^2)$ is shown in Figure 2(a) and is indicated by the symbol □. Comparing the temperature dependence of peak 1 between the experimental (open circles O) and frequency reduced (□) data, we find that they overlap except at low temperatures (< 70K). This may be indicative of the fact that the vibrational density of states $g_b(\omega)$ could be represented by $I^F(C_b \sim \omega^2)$. At this juncture, we do not want to emphasize this point and leave it open for later discussions.

The frequency reduced Raman spectra $I^F(C_b \sim 1)$ as a function of temperature are shown in Figure 5. The temperature dependence of peak 1 is shown in Figure 2(c). The $I^F(C_b \sim 1)$ spectra at all temperatures are superimposed on a sloping background which arises due to the factor $\omega/(n+1)$ in equation (3). This background has been subtracted from each spectrum in Figure 5. The frequency reduced vibrational band 1 is peaked at 80 cm^{-1}, while the center of band 2 is at around 140

cm^{-1}. The integrated intensity of band 2 is approximately 85% of that of band 1. Therefore, within experimental error, the relative integrated intensities between band 1 and band 2 are the same for the temperature reduced (I_T) and frequency reduced Raman spectra ($I^F(C_b - 1)$). Because of the weakness of band 2 in IEXP and $I^F(C_b \sim \omega^2)$, no attempt has been made to compare the relative intensities of band 1 and band 2.

IV. Discussion

A. Low frequency scattering from long wave length acoustic phonons.

The theoretical model of Martin and Brenig[7] yields an expression for Raman intensity in the low frequency region which can be expressed as follows:

$$I_{\alpha\beta\gamma\delta} \alpha C_{\alpha\beta\gamma\delta}(\omega)\, g(\omega)\, [n(\omega)+1]/\omega \qquad 4(a)$$

where the Raman coupling coefficient $C_{\alpha\beta\gamma\delta}$ is

$$C_{\alpha\beta\gamma\delta}(\omega) \alpha x^2 [g_t(x)\, E^t_{\beta\alpha\gamma\delta} + g_\ell(x) E^\ell_{\beta\alpha\gamma\delta}) \qquad 4(b)$$

Here,

$$x = 2\pi c(\omega/v_\ell)\sigma \qquad 4(c)$$

2σ = structural correlation length (SCL)

$$g_\ell(x) = \exp(-x^2) \qquad 4(d)$$

$$g_t(x) = (v_\ell/v_t)^5 \exp(-x^2(v_\ell/v_t)^2) \qquad 4(e)$$

$$E^\ell_{yzzy} = C_t^2(\delta C_t^2/C_t^2)/15 \qquad 4(f)$$

$$E^t_{yzzy} = C_t^2(\delta C_t^2/C_t^2)/10 \qquad 4(g)$$

$$E^{\ell}_{yyyy} = C_{\ell}^2(\delta C_{\ell}^2/C_{\ell}^2 + \lambda) + 4C_t^2(\delta C_t^2/C_t^2 + \lambda)/45 \qquad 4(f)$$

$$E^{t}_{yyyy} = 2C_t^2(\delta C_t^2/C_t^2 + \lambda)/15 \qquad 4(g)$$

In the low frequency region, the density of states $g(\omega)$ is assumed as the Debye density of states, i.e., $g(\omega) \sim \omega^2$. In our employed scattering geometry (HV), we only consider the term

$$C_{yzzy}(\omega) = A\omega^2 [3(v_{\ell}/v_t)^5 e^{-(2\pi c\sigma\omega/v_t)^2} + 2e^{-(2\pi c\sigma\omega/v_{\ell})^2}] \qquad (5)$$

where A is a constant. Figure 6 shows the comparison between theory and experiment. At room and higher temperatures, $(n + 1) \approx K_B T/\hbar\omega$. The intensity and the SCL can be estimated[5b] from the relation

$$2\sigma = v_t/\pi c\omega \qquad (6)$$

The velocities of transverse and acoustic waves are obtained from reference 8. From Figure 6, it is evident that the choice of $C_b \equiv \omega^2$ is not valid above 28 cm^{-1} for temperatures below T_g(573K) and 20 cm^{-1} for temperatures above T_m(723K). Using equation (6), the SCL(2σ) are estimated to be 13A, 4.1A, and 9A from the observed experimental peaks at 28 cm^{-1}(300K), 22 cm^{-1}(573K) and 10cm^{-1}(673K) respectively. The SCL's obtained from curve fitting are shown in Figure 6. Above 500 K, the SCL values are somewhat lower probably because of the choice of velocities from reference 8(b)

on the Brillouin data at 800 K. The diameter of a boroxol ring is approximately between 2-3A,the correlation range obtained from curve fitting at room temperature is somewhat larger (Figure 6) . The large value of SCL probably indicates the presence of atomic clusters that can be associated with normal vibrations of v-B_2O_3 in the low frequency region(<300 cm^{-1}). This will be discussed further in the next section.

We have decided to fit the theory of Martin and Brenig with the temperature reduced spectra instead of frequency reduced spectra is due to the presence of a quasielastic low frequency tail (Figure 4) below 70 K in the latter spectra. Although the stray light rejection in our spectrometer was reasonable - an exponential backgound was observed in the recorded spectrum at all temperatures. This background was further enhanced in the frquency reduced data as was discussed in the previous section. Above 30 cm^{-1}, we feel that either the temperature or frequency ($I^F(C_b \sim 1)$) reduced Raman data could very well represent the vibrational density of states. Comparing these two spectra between 80 and 500 K, we find that the band shapes of these two sets of data are at best,qualitatively similar; but they are not comparable to each other. Below 500K, band 1 appears at 50 cm^{-1} for $I_T(C_b \sim \omega)$, while for

$I^F(C_b \sim 1)$ it is at 80 cm^{-1}. The peak position of band 2 appears at 140 cm^{-1} in both cases. Near the glass transition temperature, band 1 in the temperature reduced spectra (Figures 2(b) and 3), shows a sharp decrease in frequency, which is also observed in the experimental Raman data (Figures 1 and 2(a)). This sharp decrease in frequency is attributed to a change in mass distribution and force constants near the glass transition temperature. This will be elucidated more in section IV-C. The frequency reduced data $I^F(C_b \sim 1)$ do not exhibit such a sharp decrease in frequency as can be seen from Figures 2(c) and 5. Therefore, this form of vibrational density of states fails to exhibit evidence for a rapid structural change near the glass transition. From the above analysis of our data, we are tempted to believe that the temperature reduced Raman spectra in which C_b varies as ω are probably the true representation of a vibrational density of states between 30 and 300 cm^{-1}.

B. Structure of v-B_2O_3

It has been reported[9] that for v-B_2O_3, the best fit to the x-ray correlation data is obtained from a glass structure comprising a mixed random network of boroxol groups and BO_3 triangles. It has been confirmed spectroscopically[1-2] that the 806 cm^{-1} peak is associated with the oxygen motion of boroxol rings. Recently, Bril[10] has reported values for various force constants associated

with different motions of the B_3O_6 ring using a free ion model. Bril studied the low frequency (26 cm^{-1}) peak as a function of composition. Assuming a mass of 130 a.m.u. for a B_2O_3 glass of 50% alkali oxide and taking the frequency of vibration to be 100 cm^{-1}, Bril estimated that the mass in question was ~ 2300 a.m.u. for this low frequency band. This corresponds to ~ 169 atoms. Therefore, he suggested that the 26 cm^{-1} band might represent the motion of a cluster of atoms. Using this estimated mass, one gets a value of 2 N/m for the force constant from the relationship: $\omega = \sqrt{k/m}$. This value is much smaller than those listed in reference 10.

With regard to the 137 cm^{-1} band, the force constant is calculated to be ~ 2.5 N/m by using the mass of a single boroxol unit (~ 80 a.m.u.). Between 8 and 673 K, the temperature reduced Raman spectra exhibited five major bands (Figure 7) which were obtained by Gaussian decomposition method with a Dupont 310 curve analyzer. It is to be noticed that at 8K,the position of the first band at 28 cm^{-1} is close to that of the theoretical band discussed in section IV A. However,the half width (HW) is larger (e.g.at 8K,the HW of the theoretical peak is 33 cm^{-1},while that of the experimental data(Figure 7(a)) is 43 cm^{-1} . From Figure 7, we find that the the ratio of the integrated intensity between the 62

cm^{-1} and 131 cm^{-1} band is .656. Assuming that this ratio reflects the concentration ratio (N_1/N_2) between the BO_3 triangular network and boroxol rings, and using $N_1 + N_2 = 1$, we estimate N_1 and N_2 as 40% and 60%, respectively. At 673K, these two concentrations are estimated to be 45% and 55% respectively. Therefore, the decrease in intensity of the 131 cm^{-1} band (or 137 cm^{-1} band in Figure 3) above T_g may be associated with the breakdown of boroxol rings. It is also found[1(b)] that the peak height of the 131 or (137 cm^{-1}) band decreases considerably in molten B_2O_3. It is our belief that the 137 cm^{-1} band in the temperature reduced spectra is partly due to the librational motions of boroxol rings. This assertion will be further confirmed when we discuss our high pressure data in the ensuing section.

We now intend to describe a structural model for the B_2O_3 glass. A recently proposed model of v-B_2O_3 by Johnson and co-workers[9] indicated that at room temperature there was likely to be an equal concentration of boroxol rings and BO_3 triangles. A random boron-oxygen network with a high proportion of boroxol rings is shown in Figure 8(a). This two dimensional network can be extended to a three dimensional one by assuming that BO_3 triangles of all orientations are interconnected in space to form a three dimensional network. It is assumed that cage like structures (as shown by shaded areas in Figure (8a)) of various shapes

and sizes can be constructed in v-B_2O_3 and this random distribution of mass simulates the disorder in the glassy state. It has been shown by Payton and Vischer[11] that in mixed diatomic crystals, the calculated vibrational density of states corresponding to acoustic and optic modes overlaps when the force constants and masses are chosen randomly. In diatomic crystalline solids, the acoustic and optic modes are defined, respectively, as in-phase and out-of-phase motions of atoms. The two observed bands at 50 cm^{-1} and 137 cm^{-1} may then be ascribed to these two type of motions. Bell and co-workers[6(c)] used the BO_3 triangular network as well as boroxol ring configurations to perform the vibrational analysis of B_2O_3. They estimated bond stretching, out-of-plane bending and O-B-O angle bending constants in both configurations. Their results based on the boroxol ring model produced a vibrational density of states which has the correct band shape; but failed to agree with the observed peak positions in the Raman data. Galeener et. al.[4] also attempted to obtain a vibrational density of states using a nearest neighbor force constant model with a continuous BO_3 triangular network configuration. However, their calculations were unable to achieve the observed Raman peaks. We believe that the 806 cm^{-1} peak is an internal mode associated with the boroxol rings while the vibrational features which appear below 300 cm^{-1} are due to cooperative

motions of the whole structure, comprising a mixed BO_3 triangular and boroxol ring network. Therefore, a lattice dynamical calculation, following a similar kind of model used by Bell and co-workers and Payton et. al., is warranted at this stage to reproduce the Raman data. A much smaller central force constant with a random distribution of mass may be a good starting choice. The vibrational density of states could be obtained from such calculations.

Above T_g and in the liquid state, it has been established that a random open structure is formed by a reorganization of BO_3 triangles from boroxol groups. This is shown in Figure 8(b). In our Raman data as a function of temperature, we observe a shift in the Raman spectra to the low frequency side above T_g(573K). Above T_m(723K), the vibrational spectrum shifts very slightly in frequency[1b] (Figure 2). The change in frequency near T_g is attributed to a sudden change in structure, resulting in a weaker force constant. This assertion will be further discussed in the next section.

C. Glass Transition

A glass transition is normally manifested by a marked change in viscosity, specific heat and thermal expansion cofficient within a narrow temperature interval. The glass transition temperature is defined as the temperature at which the viscosity of the material becomes very high (>10^{13}Poise). The glassy state is considered to be an extension of the liquid

state and is regarded as a disordered solid. It is important to mention that the high temperature side of the glass transition is nothing more than the liquid state. The transition between liquid to glassy state may be a thermodynamic phase transition, or a phase transition that is observed by kinetic effects, or no phase transition at all. At the beginning we must decide upon a model system that describes the glass transition temperature. Although various different models exist in the literature[12], we will mainly consider two models: the lattice model by Gibbs and DiMarzio[13], and the free volume model by Cohen and co-workers[14].

i. Lattice Model

The Gibbs-Dimarzio theory deals with the glass forming linear polymer chains each containing a backbone unit. The rotation of the single bonds around this backbone unit is hindered and this gives rise to potential wells in the rotational space separated by different barrier heights. The bond spends almost all of its time librating around the minimum of one or another of the potential wells. A configurational state is assigned to describe the state of the whole system and it is assumed that below T_g, the whole system is frozen into one configurational state i.e. in one such minimum. Above T_g, the liquid state

explores the possibility of settling into higher configurational states. Each configurational state is associated with a set of vibrational and librational states which are the internal modes of the system. Goldstein[15] used a different kind of molecular mechanism which rests on the following assumptions: (1) The heights of the potential minima associated with different configurational states are sufficiently close to each other, and at a temperature near T_g, the system remains trapped in one of the minima; (2) the lattice vibrational properties are characterized by a Debye characteristic frequency, which is a function of temperature; (3) the lattice frequencies could change at higher temperatures because the potential minima associated with different configurational states might have different curvatures; (4) a change in anharmonicity occurs at high temperatures with changing structural states.

We now try to relate the above findings to interpret our Raman data. We assume that the cages containing clusters of atoms shown by the shaded areas in Figure 8(a) are librating. They are trapped in one of the potential wells below T_g and the librational motions of clusters of atoms of

various sizes may be responsible for the observed low frequency peaks in the calculated Raman density of states. The force constants associated with the 50 cm^{-1} and 137 cm^{-1} peaks are comparable to each other and therefore, it may not be incorrect to say that these librational motions are probably decoupled motions around the center of mass of each cage. The momentum should be conserved in the whole system and this requirement may be achieved by making suitable combinations of clockwise and anticlockwise librations. With increasing temperature, the large amplitude of motions of individual bonds would broaden the vibrational spectrum; but the vibrational density of states should not change unless the structure is changed. This was indeed observed as is indicated in Figure 2.
Above 500K and near T_g, a number of boroxol rings are broken extending the polymeric network of the BO_3 triangles, thereby decreasing the density of atoms. Therefore, there will be a weakening of the force constants between atoms. Since the potential wells are closely spaced together, the system would seek a new equilibrium position at a different configurational state. The potential minima associated with the different

configurational states are likely to have different curvatures, mostly weaker parabolas because of the weakening of force constants. All these effects would result in a shift of the scattering spectra to lower frequencies. However, we find[1b] that the experimental as well as the frequency and temperature reduced Raman spectra do not exhibit a marked shift in frequency above the melting point T_m(723K) of the B_2O_3 glass. Above T_m, the scattering spectrum peaks at a lower frequency (Figures 2a,b,c) and very little shift was observed at higher temperatures. This may be explained from the fact that at high temperature, the viscosity of the melt is lowered and instead of linking the ruptured bonds of boroxol rings to the same network, which would result in a larger mass and therefore, a lower frequency which is not observed, one can think of regrouping of atoms, leading to a more open structure (Figure 8b). These clusters of atoms are still harmonically bound to their neighbors but with a much weaker force constant than the glassy state. As the temperature is further raised, the number of these cluster of atoms increases, while the number of boroxol rings decreases. The integrated intensity of the whole contour below 300 cm^{-1}, however, will remain

constant unless there is a marked change in free volume. The integrated intensity of the vibrational density of states below 300 cm^{-1} was indeed found[1(b)] to be constant. It is argued that although the specific volume data of Marcedo and co-workers[16] indicated about a 14% change in free volume, which would result in a decrease of the intensity of the low frequency band, it might not be discernible by Raman experiments. It is worthwhile to mention at this point that the Brillouin [8(b)] and hypersonic sound [16(b,c)] scattering data also exhibited a sharp decrease in longitudinal,shear and bulk modulii near the glass transition temperature; but above the melting point, only a slight increase of these quantities was observed.

ii. Free Volume Model

The Cohen-Turnbull theory considers molecules as being trapped in a cage or cell by its nearest neighbors. In the liquid state the motion of the molecules is regarded as kinetic in the inner part and vibrational in the peripheral of this cage. These molecular cells could be either liquid like or solid like. Near $T \to 0$, only solid like cells exist; but near T_g, cells of both types

co-exist. A liquid like cluster is defined as a cluster containing liquid like cells and a free volume is available to these cells whenever the local volume (V_m) of these cells exceeds a critical volume (V_c). The molecules can diffuse continually whenever the fluctuation in V_m is $>V_c$. The free volume model predicts a first-order phase transformation from a liquid to glassy state, depending on the thermal history (i.e. slow heating or cooling) of the sample. It also describes a process in which a condensation of the free volume into vacancies is postulated during the cooling of a liquid. A tunneling mechanism between voids is predicted by this model, which would give rise to a quasi elastic scattering in Raman experiments.

This model lends support to our conjecture of the previous section where we described that above T_m, a regrouping of atoms occurs which would eventually lead to an open random structure of various ring sizes as depicted by Figure 8(b). We also believe that in the liquid state, a cage like structure still prevails and the motions are partly kinetic and partly vibrational as described by this model. However, we were unable to determine from our Raman data whether the glass-liquid phase

transformation is of first or second order.

V. Discussion of the Pressure Dependence

In Figure 9, we show the low frequency Raman spectra as a function of pressure. The temperature reduced Raman spectra are shown in Figure 10. It is to be noticed that the experimental Raman data only show a broadening of the vibrational band as a function of pressure, while the temperature reduced spectra exhibit a shift in frequency. The frequency reduced Raman spectra I_F ($C_b \sim \omega^2$) do not reflect the frequency shift as a function of pressure and are not shown. The $I_F(C_b \sim 1)$ spectra are associated with a strong linear background with increasing frequency at high pressure, thereby masking any discernible features. The shift of the vibrational band at high pressure reflects compression-induced changes in the intermolecular forces, and one would expect the vibrational band to be shifted to the high frequency side under compression as was observed for the 50 cm^{-1} band in the temperature reduced Raman spectra. This observation confirms our assertion made earlier in section IVA that the vibrational density of states of v-B_2O_3 is best represented when C_b is assumed to vary as ω.

For a given mode i, the mode Gruneissen parameter γ_i is related to the fractional change in frequency as:

$$\gamma_i = \frac{B_T}{\omega_i} \quad \frac{\Delta\omega}{\Delta P} \qquad (7)$$

where B_T is the bulk modulus.

Table 1 lists the shift in vibrational frequencies of the temperature reduced Raman spectra as a function of hydrostatic pressure. A Gaussian decomposition of the spectra is shown in Figure 11. The peak position of the 806 cm^{-1} peak was obtained from the experimental data and was found unshifted upon compression. It is worthwhile to mention that this peak is also insensitive to the temperature as regard to its peak position. The observation of no change in peak position of the 806 cm^{-1} peak under compression is indicative of the fact that the external pressure is acting on the oxygen of the BOB unit thereby reducing the bond angle which in turn pulls the extra annular oxygen away from the boroxol ring (Fig. 8). This would result in a decrease in the force constant for the librational motion of the boroxol ring, giving a negative γ. However, the B-B distances become shorter upon external pressure and a cooperative in-phase acoustic type of motion of the atoms would experience large repulsive forces which would result in higher effective force constant. Hence a positive γ will be expected as was observed for the 50 cm^{-1} band. The Gaussian deconvoluted band (Figure 8) indicates a negative shift in frequency for the 123 cm^{-1} and 206 cm^{-1} bands which implies that both of them are probably associated with the librational motions(e.g. the second peak may be associated with a combination band) of boroxol rings.

We have also calculated the volume thermal expansion coefficient α from the pressure dependent Raman data. The volume thermal expansion coefficient α is related to the change in entropy as:

$$\alpha = \frac{1}{V} \left(\delta V/\delta T \right)_P = - \frac{1}{V} \left(\delta S/ \delta P \right)_T \qquad (8)$$

If the density of states $g(\omega, p)$ is known as a function of pressure, the entropy can be determined from the following relationship:

$$S(P,T) = \frac{S(\omega,T)\ g(\omega,P)\ d\ \omega}{g(\omega,P)\ d\ \omega} \qquad (9)$$

Assuming a quasi-harmonic theory in which vibrations are regarded as harmonic, the entropy function is expressed as:

$$S(x) = K_B \left[\left\{ \frac{x}{(\exp(x) - 1)} \right\} - \ln\{ 1 - \exp(-x) \} \right] \qquad (10)$$

where $x = h\omega/K_B T$, K_B is the Boltzman constant.

We have used experimental as well as temperature reduced Raman data as the vibrational density states to perform the entropy integration as is shown by equation (9). The integration was perfomed numerically between 12 and 900 cm^{-1} at an interval of 1 cm^{-1}. The changes in entropy for the experimental and temperature reduced Raman spectra are estimated to be -.229 R and -.12 R respectively, where R is 8.052 x 10^{-2} lit atm/ K mole using v=.5548

g/cm^3 from reference 16(a), we estimate $\alpha_{EXP}=6.15\times10^{-5}$/ K and $\alpha_T=3.2\times10^{-5}$/ K, respectively, for the experimental and temperature reduced Raman data. Macedo et al[16] reported the value of α as 4.2×10^{-5}/ K at room temperature. Remembering that we performed the integration from 12 cm^{-1}, α_T is probably the right choice which again lends support to our previous assertion that the temperature reduced spectra truely represent the vibrational density of states.

Conclusions

Low frequency Raman data as a function of temperature and pressure were used to determine the structure of v $-B_2O_3$. At room temperature, a structure comprising equal proportions of BO_3 triangles and boroxol rings is postulated. A true representation of the vibrational density of states of this system is found to be dependent on the Raman coupling coefficient C_b. We find that C_b varies as ω^2 below 30 cm^{-1} and as ω between $30<\omega<300$. The two observed vibrational bands at 50 and 137 cm^{-1} are ascribed to in-phase and out-of phase motions arising from a random distribution of mass and ring size of the structure. We find that a correlation length of 10 A fits our data at room temperature and below which implies that the low frequency vibrational bands are associated with motions of atomic clusters (i.e larger rings than boroxol units).

It is also concluded from the temperature and pressure dependent data that the 137 cm^{-1} band is associated with librational motions of boroxol rings. Near T_g, the observed shift in frequency of the vibrational spectra is attributed to the weakening of the force constant due to "break down" of boroxols leading gradually to a more open random network structure consisting mainly of BO_3 triangles.

References

1. (a) G.E. Walrafen, S.R. Samanta and P.N. Krishnan, J.Chem Phys., 72, 1 (1980)

   (b) G.E. Walfrafen,M.B.S Hokmabadi,P.N.Krishnan and S. Guha.,J.Chem. Phys(to be published)

2. C.F. Windisch, Jr. and W.M. Risen Jr., J. Noncrystalline Solids, 48, 307 (1982)

3. (a) R. Shuker and R.W. Gammon, Phys. Rev. Letters, 25,222 (1970)

   (b) R. Shuker and R.W. Gammon, J. Chem. Phys, 55,4784 (1971)

4. F.L. Galeener, G. Lucovsky and J.C. Mikkelson Jr., Phys. Rev. B., 22, 3983 (1980)

5. (a) J. S. Lanin, Solid State Comm.,12,947,(1973)

   (b) R. J. Nemanich, Phys. Rev. B., 16, 1655,(1977)

   (c) Other relevant references could be found in the article by J. Jackle, pp 135 in "Low temperature properties", Ed. W. A. Phillips, Springer-Verlag(1981) and references therein.

6. (a) R. J. Bell, N.F. Bird and P. Dean, J. Phys. C, 7, 2457 (1974)

   (b) R.J.Bell,A.Carnavile,C.R.Kurkjian,G.E.Peterson,J.Non-crystalline Solids,35-36,1185 (1980)

   (c) R.J.Bell and A. Carnavile,Phil.Mag B,43,380 (1981)

7. A.J. Martin and W. Brenig, Phys. Status Solidi, b64, 163 (1974)

8. (a) J. Pelous, Physics letter, 74A, 275 (1979)

(b) J.A. Bucaro and H.D. Dardy, J .Appl. Phys., 45, 2121 (1974) ; At 800K, $v_\ell = 2.025 \times 10^5$ cm/sec and $v_t = .85 \times 10^5$ cm/sec

(c) The transverse velocity at low temperature was estimated from the relationship:

$$\frac{1}{v_{DEB}^3} = \frac{1}{v_\ell^3} + \frac{1}{v_t^3}$$ where $v_D = 2.04 \times 10^5$ cm/sec and $v_\ell = 3.48 \times 10^5$ cm/sec

9. (a) P.A.V Johnson, A.C. Wright and R.N. Sinclair, Report to be published in AERE-R10173, C14, August (1981)

(b)R.N.Sinclair,J.A.Desa,G.Etherington,A.C.Wright,J.Non Crystalline Solids,42,107 (1980)

10. T.W. Bril, Phillips Res. Reports, Suppl. No.2 (1976)

11. D.N. Payton and W.M. Visher, Phys. Rev.,175, 1201 (1968)

12. Structure and mobility in molecular and atomic glasses, Ed. J.M. O'Reilly and M. Goldstein, The New York Academy of Sciences (1981)

13. E.A. DiMarzio and J.H. Gibss, J.Chem Phys., 28,807 (1958)

14. M.H. Cohen and G.S. Grest, Phys. Rev. B,20,1077 (1979)

15. M. Goldstein, J. Chem. Phys., 67, 2246 (1977); ibid J. Chem. Phys, 64, 4767 (1976)

16 (a) P.B. Macedo, W. Capps, and T.A. Litovitz, J. Chem. Phys, 44,3357 (1966)

(b) W. Capps,P.B.Macedo,B.O'Meara and T. Litovitz,J.Chem.Phys. 45,3431 (1966)

(c) N. Goldblatt, R. Figgins,C.J.Montrose and P.B.Macedo, Physics and Chemistry of Glasses,12,15(1971)

Lists of Figures

Figure 1: Experimental Raman spectra (IEXP) in the low frequency region (< 300 cm^{-1}) at different termperatures. Slit widths of 4 cm^{-1} were employed.

Figure 2: A plot of shift in frequency vs. temperature for (a) experimental (IEXP) Raman data indicated by open circles (o); frequency reduced intensity I^F ($C_b \sim \omega^2$) indicated by squares (□), (b) temperature reduced intensity ($I_T(C_b \sim \omega$) indicated by full circles (•) and (c) frequency reduced intensity ($I^F(C_b \sim 1$) indicated by Ø. The frequency scale in parenthesis () is applicable only for (c). Here T_G and T_M are the glass transition and melting point temperature.

Figure 3: Temperature reduced Raman intensity ($I^T(C_b \sim \omega$) at different temperatures. A background has been subtracted from each spectrum.

Figure 4: Calculated reduced spectral density of states $I^F(C_b \sim \omega^2)$ at different temperatures.

Figure 5: Calculated spectral density of states $I^F(C_b \sim 1)$ at different temperatures. A sloping background has been subtracted from each spectrum.

Figure 6: Comparison between theory (dashed line) and experiment

(solid line). The structural correlation length is 2σ.

Figure 7: Gaussian decomposition of the temperature reduced Raman data. No background subtraction has been done.

Figure 8: (a) A possible B_2O_3 structure at room temperature containing a high proportion of boroxol rings. Here the cluster of atoms which,we believe, may be responsible for the low frequency Raman spectrum is shown by shaded areas. A possible librational motions of these clusters is shown by arrows.
(b) The B_2O_3 structure in the molten states containing only BO_3 units. It is to be noted[1c] that the density of this layered structure is approximately reduced by 3/8 th from that of (a)[6c] due to replacement of boroxol units with BO_3.

Figure 9: Experimental Raman data as a function of pressure.

Figure 10: Temperature reduced Raman data as a function of pressure. A sloping background has been subtracted.

Figure 11: Gaussian decomposition of the temperature reduced Raman data. No background has been subtracted.

Table 1: Pressure dependence of the vibrational frequencies. Here γ_i is the mode Gruneisen parameter. The Bulk modulus (B_T) is taken as 136.8 kbar from ref.4.

Pressure (kbar)	Frequency (cm^{-1})	$\frac{1}{\omega}\frac{\Delta\omega}{\Delta P}$	γ_i
0	50		
6	60	.025	+3.42
8	60		
0	140		
6	134	-.015	-2.05
8	122.5		
0	806	-	-
6	806	-	-
8	806	-	-

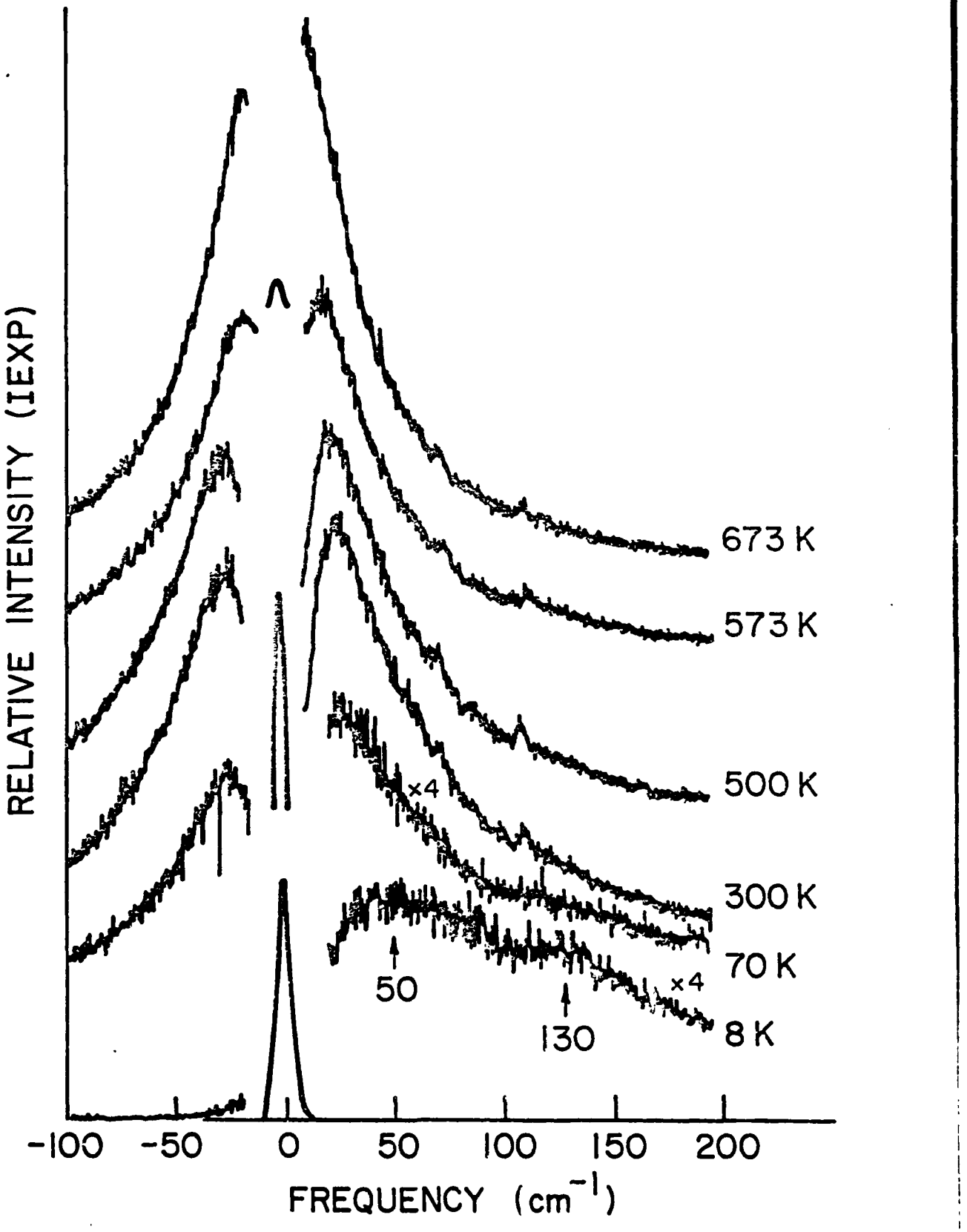
RELATIVE INTENSITY (IEXP)
673 K
573 K
500 K
300 K
70 K
8 K
×4
×4
50
130
-100
-50
0
50
100
150
200
FREQUENCY (cm⁻¹)

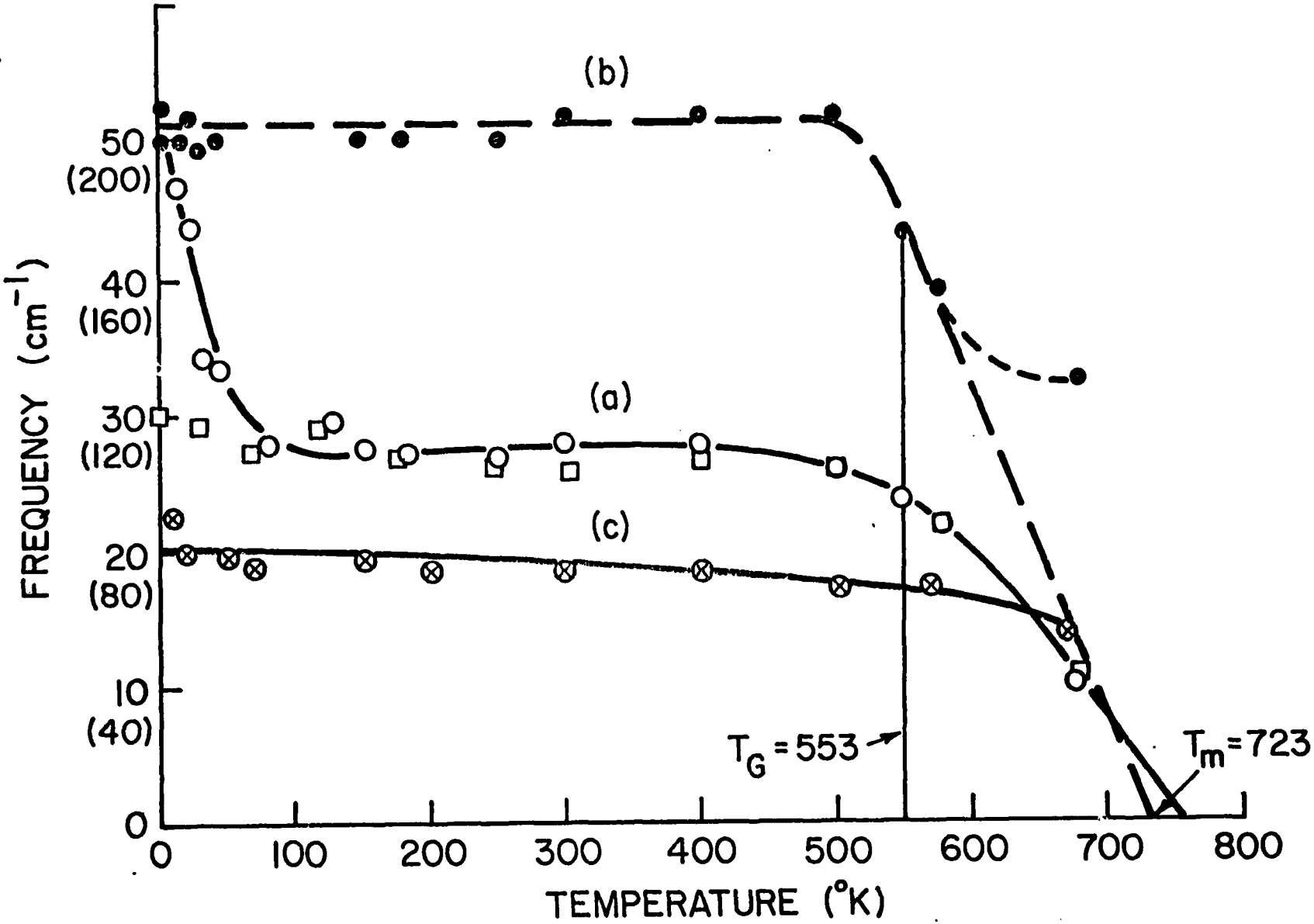
(b)
(a)
(c)
50
(200)
40
(160)
30
(120)
20
(80)
10
(40)
0
FREQUENCY (cm⁻¹)
$T_G = 553$
$T_m = 723$
0
100
200
300
400
500
600
700
800
TEMPERATURE (°K)

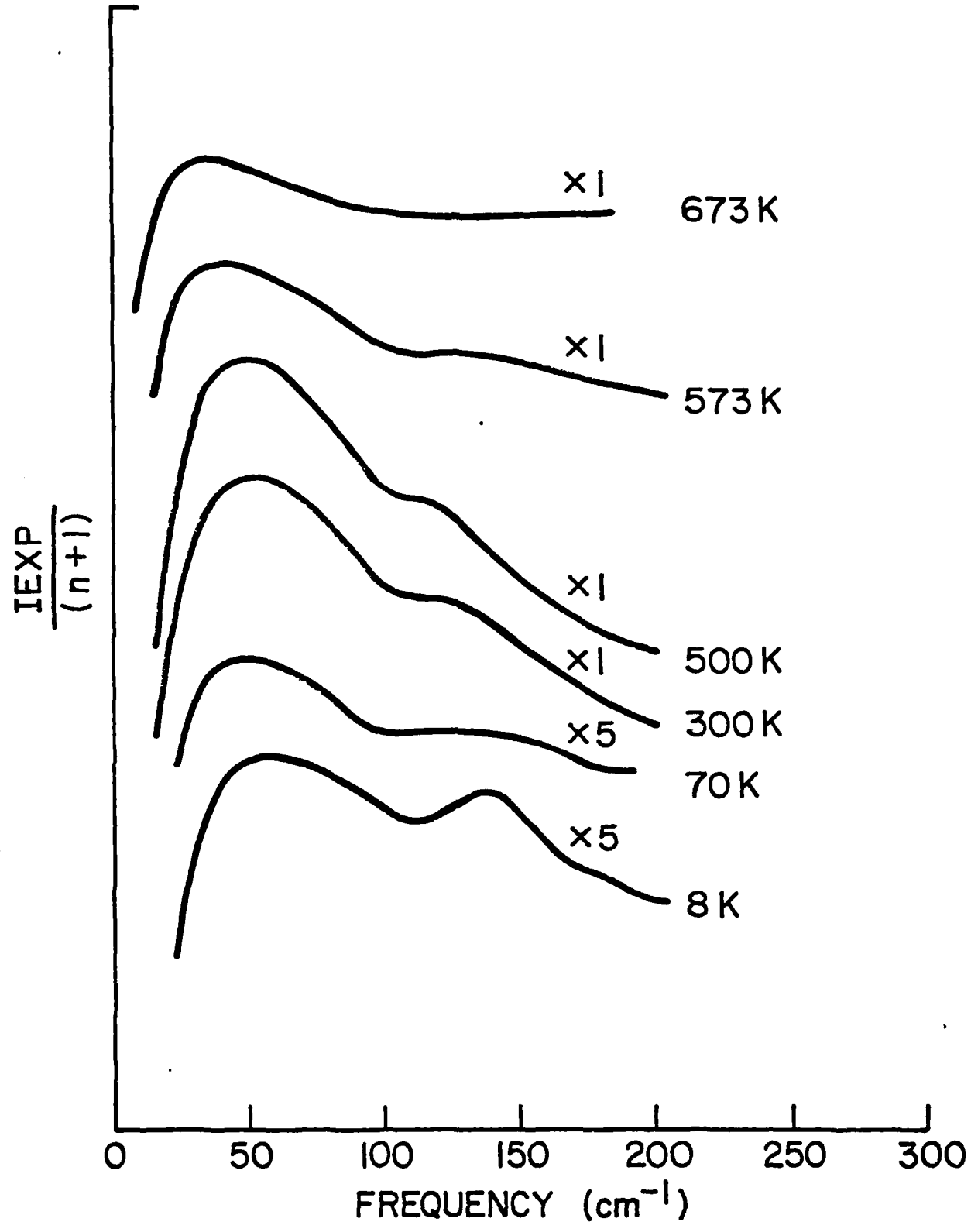
IEXP/(n+1)
×1
673K
×1
573K
×1
500K
×1
300K
×5
70K
×5
8K
0
50
100
150
200
250
300
FREQUENCY (cm⁻¹)

Fig 3

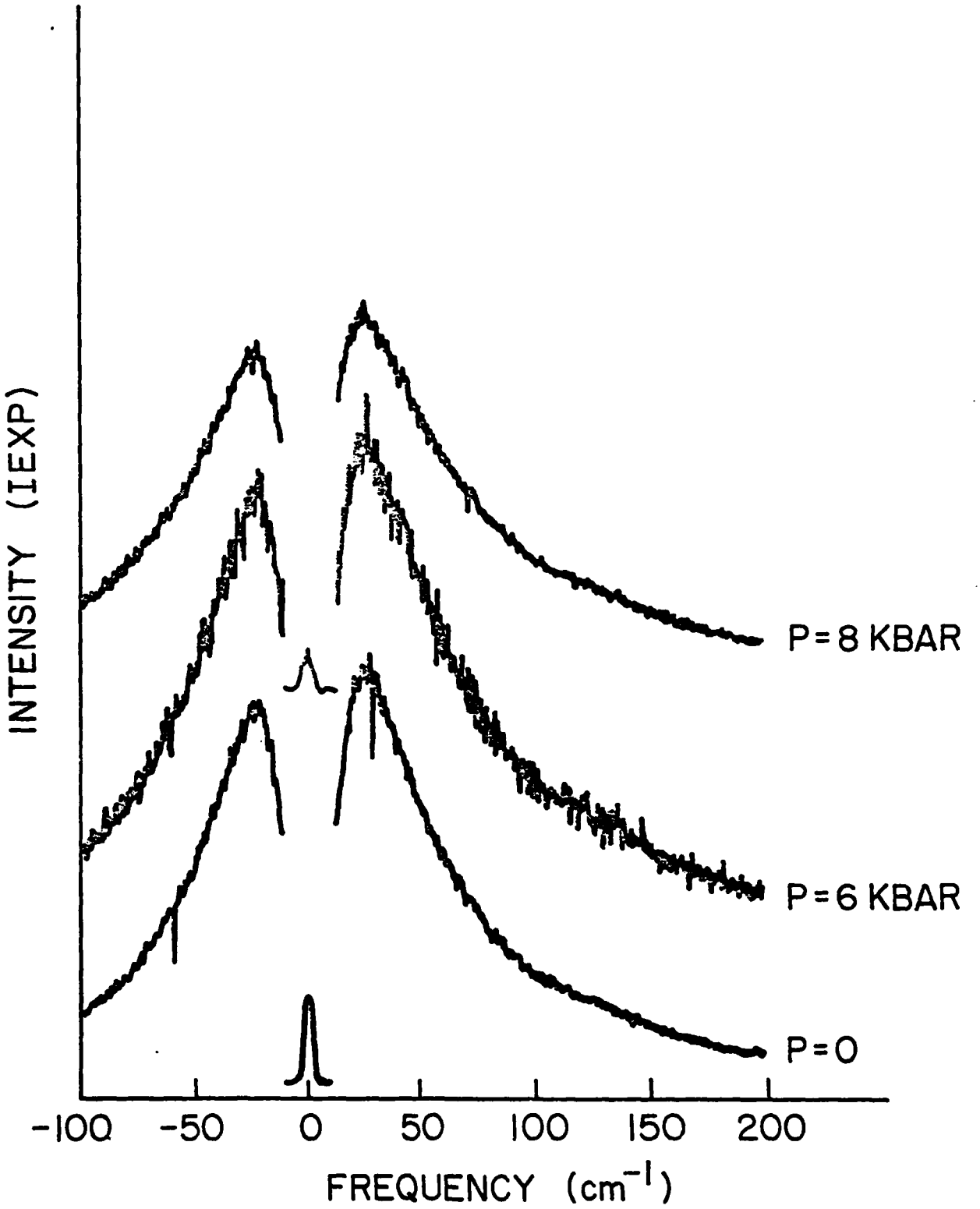
INTENSITY (IEXP)
P=8 KBAR
P=6 KBAR
P=0
-100
-50
0
50
100
150
200
FREQUENCY (cm^{-1})

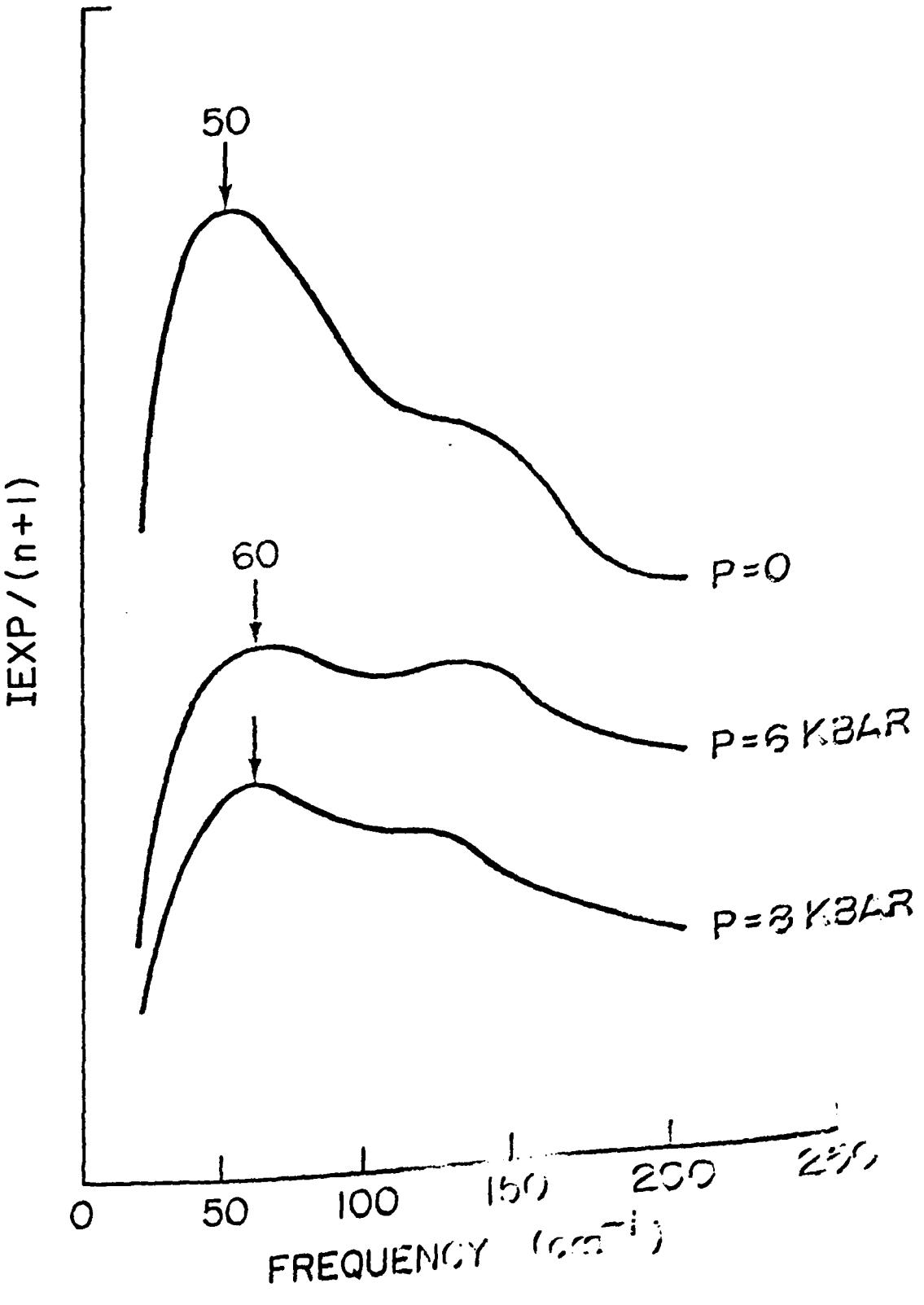
50
60
P=0
P=6 KBAR
P=8 KBAR
IEXP/(n+1)
0
50
100
150
200
FREQUENCY

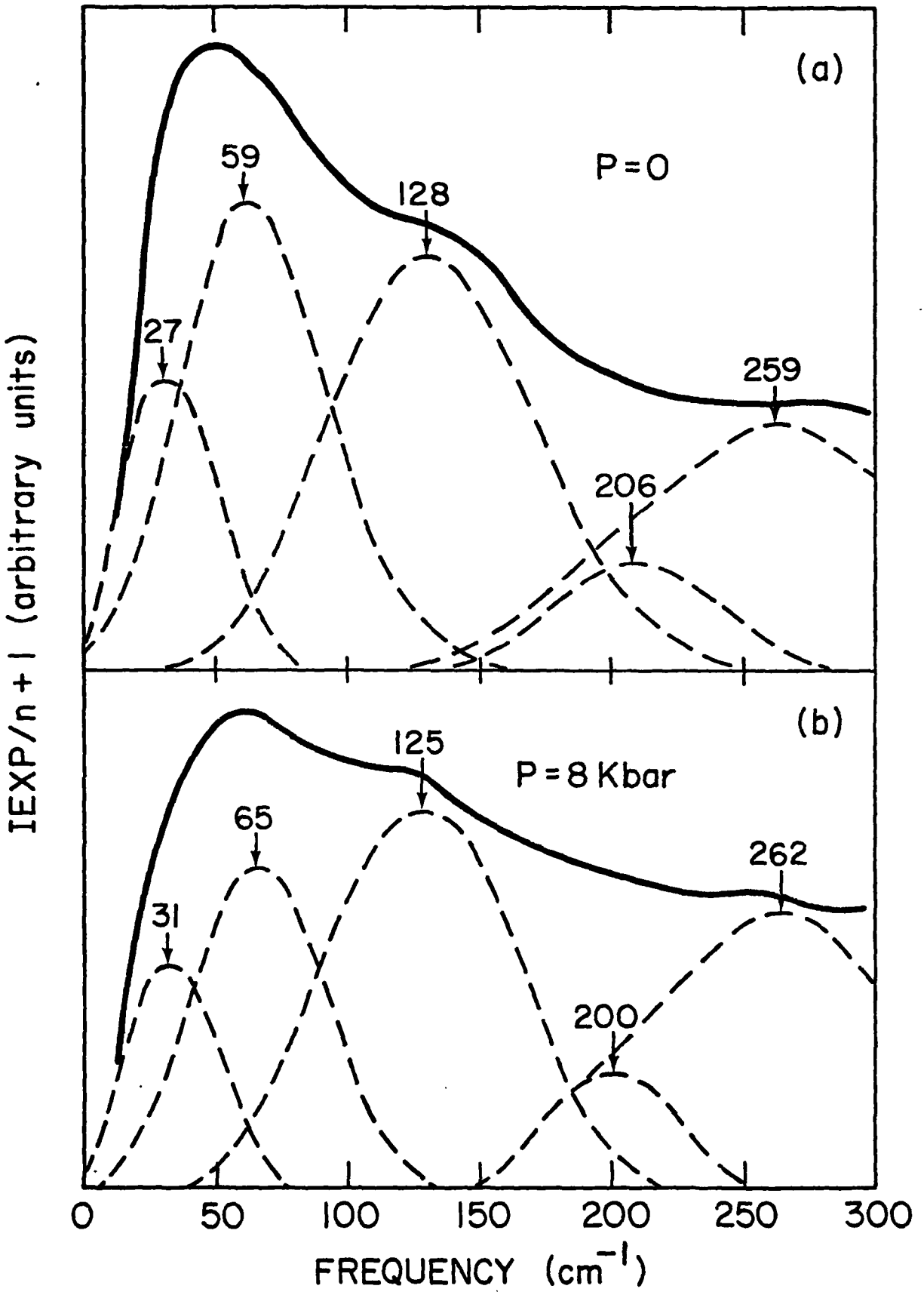
(a)
P=0
59
128
27
259
206
(b)
P=8 Kbar
125
65
262
31
200
IEXP/n+1 (arbitrary units)
0
50
100
150
200
250
300
FREQUENCY (cm⁻¹)

Fig 11

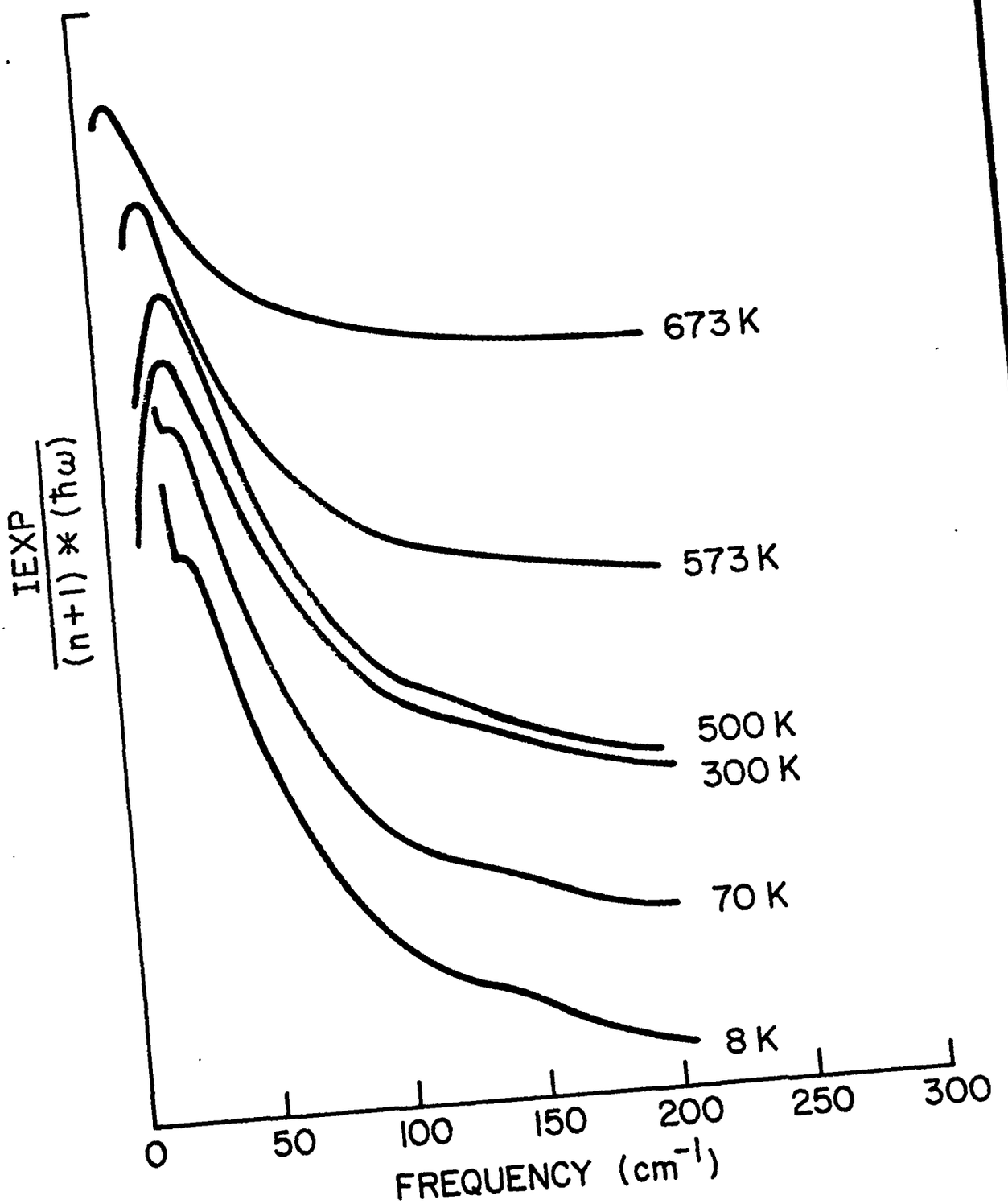
673 K
573 K
500 K
300 K
70 K
8 K
IEXP / (n+1) * (ħω)
0
50
100
150
200
250
300
FREQUENCY (cm⁻¹)

Fig 4

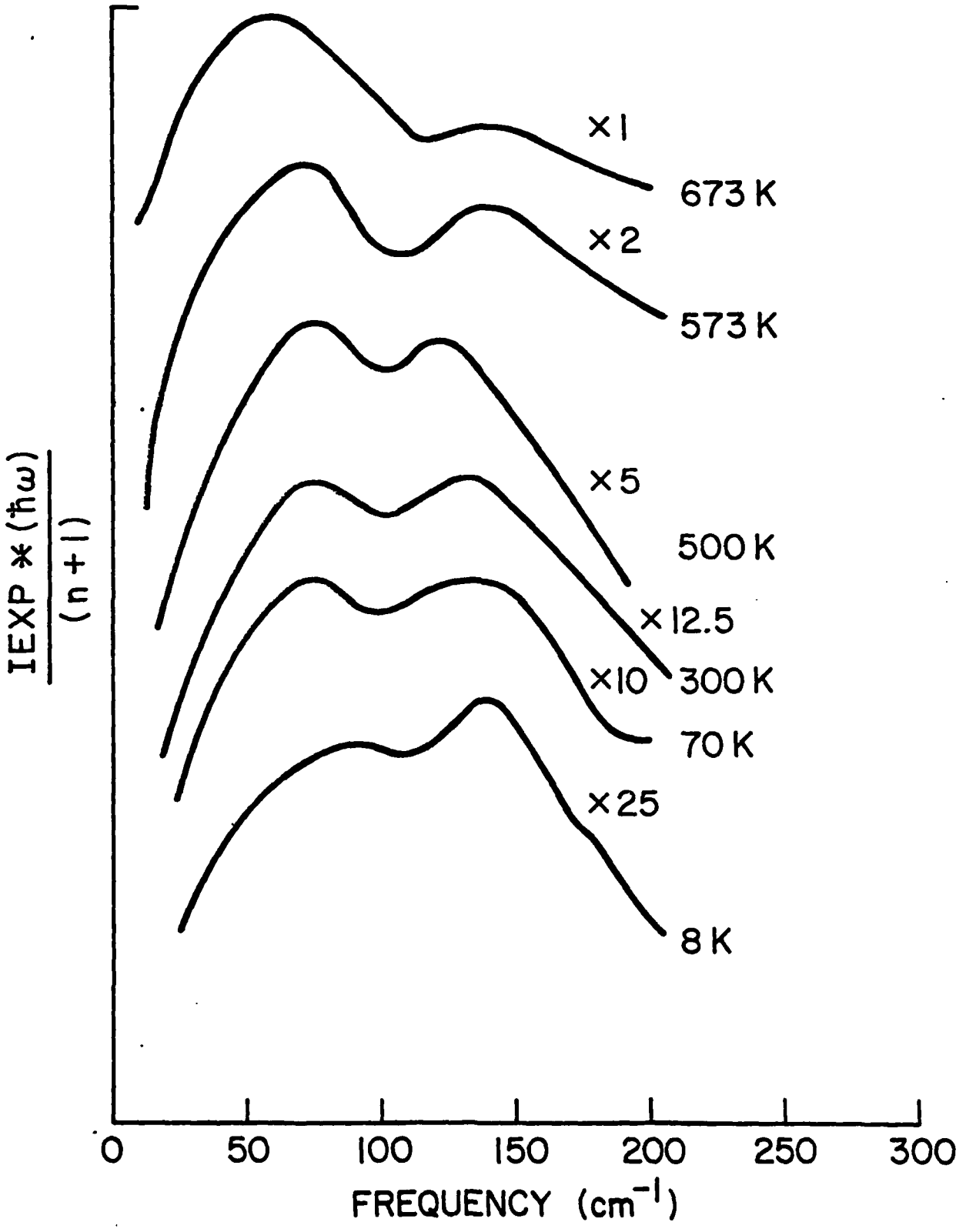
IEXP * (ħω) / (n+1)
×1
673 K
×2
573 K
×5
500 K
×12.5
300 K
×10
70 K
×25
8 K
0
50
100
150
200
250
300
FREQUENCY (cm⁻¹)

Fig 5

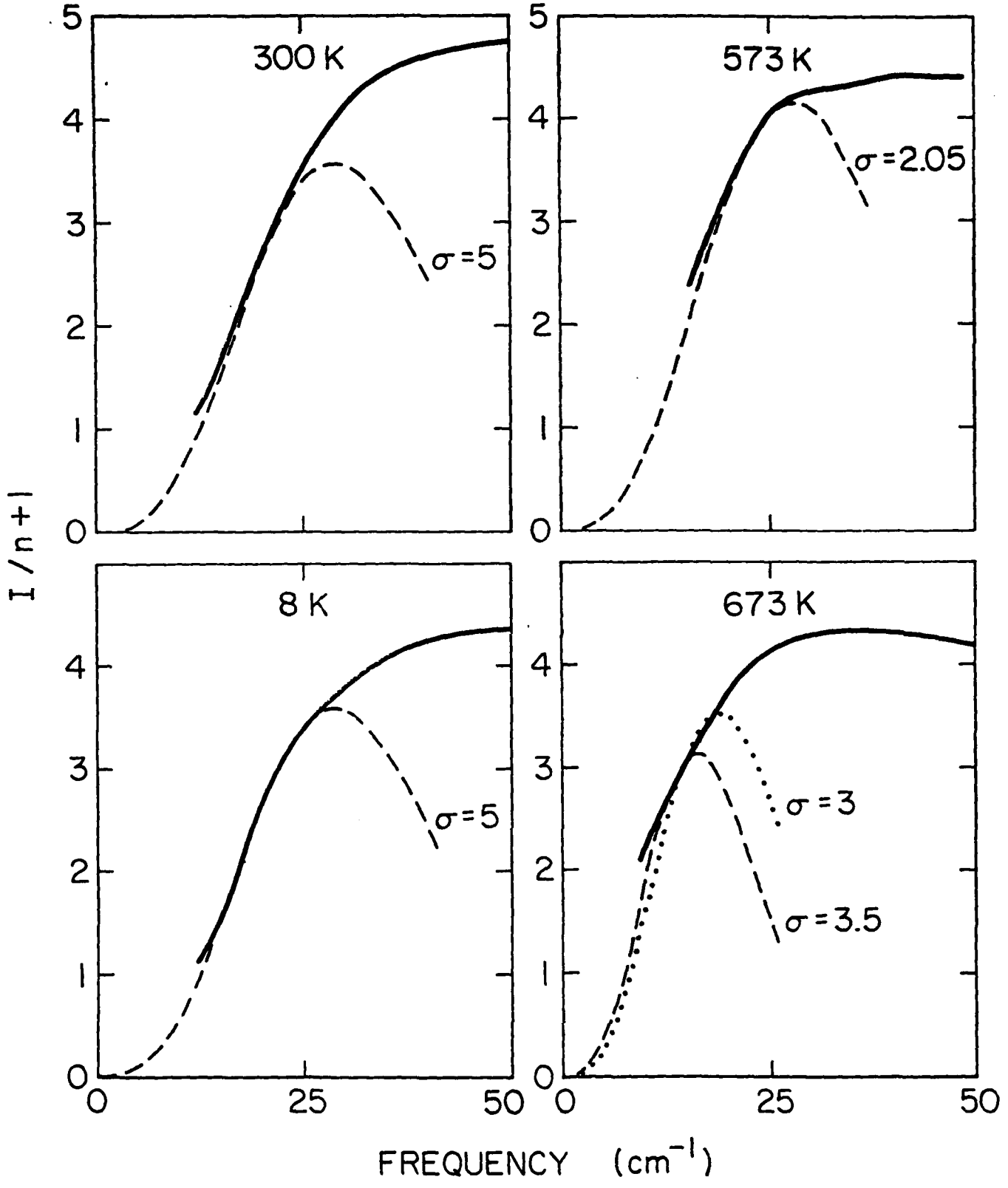
300 K
573 K
8 K
673 K
σ=5
σ=2.05
σ=5
σ=3
σ=3.5
I/n+1
FREQUENCY (cm⁻¹)
0
1
2
3
4
5
0
25
50

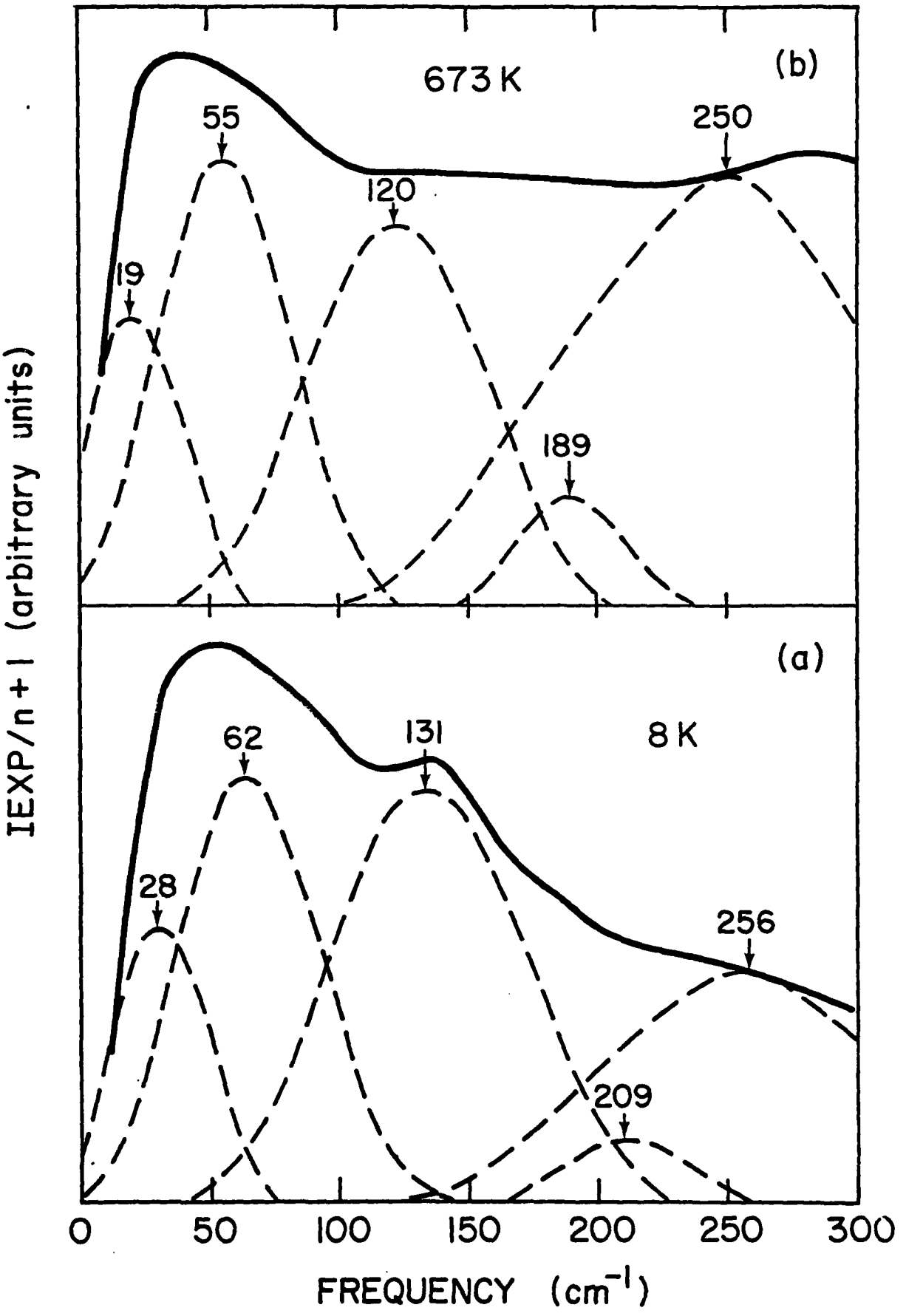
673 K
(b)
55
250
120
19
189
(a)
8 K
62
131
28
256
209
IEXP/n+1 (arbitrary units)
0
50
100
150
200
250
300
FREQUENCY (cm⁻¹)

Fig 3

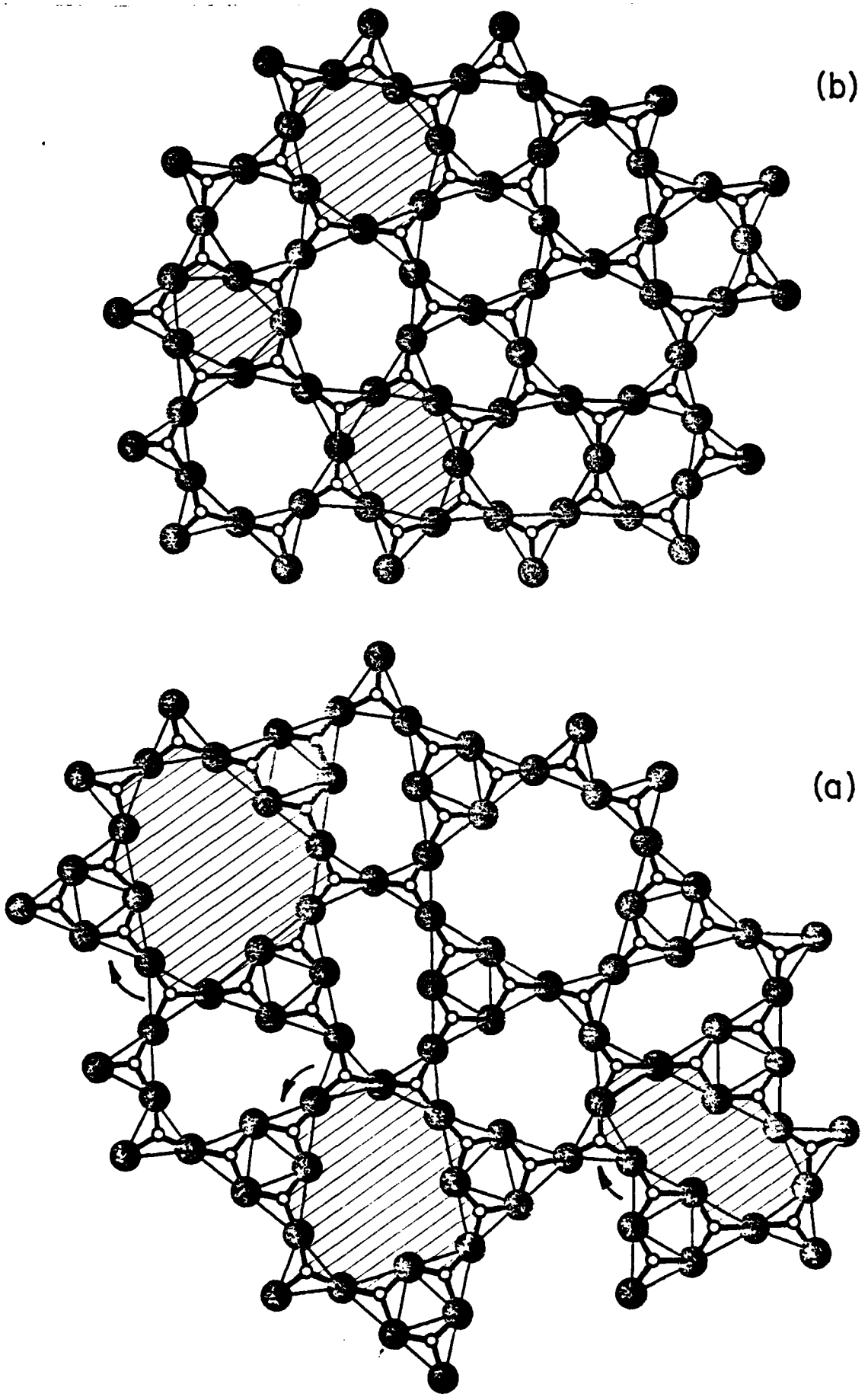
(b)
(a)

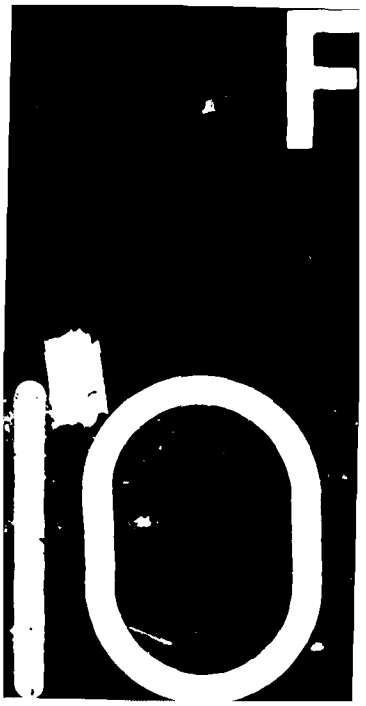
F
10